Published by Institute of Physics Publishing for SISSA/ISAS

Received: *July 26, 2003*
Revised: *August 9, 2003*
Accepted: *September 11, 2003*

Prediction of U_{e3} in neutrino mass matrix with two zeros

Mizue Honda, Satoru Kaneko and Morimitsu Tanimoto

Department of Physics, Niigata University
Ikarashi 2-8050, 950-2181 Niigata, Japan
E-mail: mizue@muse.sc.niigata-u.ac.jp, kaneko@muse.sc.niigata-u.ac.jp, tanimoto@muse.sc.niigata-u.ac.jp

Abstract: We have discussed predictions of $|U_{e3}|$ and J_{CP} in the framework of the neutrino mass matrix with two zeros. In the case of the best fit values of $\tan^2\theta_{12}$, $\tan^2\theta_{23}$, $\Delta m^2_{\rm sun}$ and $\Delta m^2_{\rm atm}$, the prediction of $|U_{e3}|$ is $0.11 \sim 0.14$. The lower bound of $|U_{e3}|$ is 0.05, which depends on $\tan\theta_{12}$ and $\tan\theta_{23}$. We have investigated the stability of these predictions taking account of small corrections to zeros, which may come from radiative corrections or off-diagonal elements of the charged lepton mass matrix. The lower bound of $|U_{e3}|$ comes down considerably due to the small corrections to zeros.

Keywords: Neutrino Physics, CP violation.

JHEP09(2003)028

Contents

1. **Introduction** 1

2. **Predictions of texture two zeros** 2

3. **Stability of predicted $\mathbf{U_{e3}}$** 5

4. **Summary** 12

1. Introduction

In recent years empirical understanding of the mass and mixing of neutrinos have been advanced [1]–[3]. The KamLAND experiment selected the neutrino mixing solution that is responsible for the solar neutrino problem nearly uniquely [4], only large mixing angle solution. We have now good understanding concerning the neutrino mass difference squared ($\Delta m^2_{\rm atm}$, $\Delta m^2_{\rm sun}$) and neutrino flavor mixings ($\sin^2 2\theta_{\rm atm}$, $\tan^2\theta_{\rm sun}$) [5]. A constraint has also been placed on the mixing from the reactor experiment of CHOOZ [6].

The texture zeros of the neutrino mass matrix have been discussed to explain these neutrino masses and mixings [7]–[9]. Recently, Frampton, Glashow and Marfatia [10] found acceptable textures of the neutrino mass matrix with two independent vanishing entries in the basis of the diagonal charged lepton mass matrix. The KamLAND result has stimulated the phenomenological analyses of the texture zeros [11]–[14]. These results favor texture zeros of the neutrino mass matrix phenomenologically.

However, there are theoretical problems. The first one is the effect of radiative corrections. A specific texture of the lepton mass matrix is not preserved to all orders. For example, non-zero components may evolve in zero-entries of the mass matrix at the low energy scale due to radiative corrections even if the zero texture is realized at the high energy scale. The second one is the choice of the flavor basis. In the model with some flavor symmetry, zeros of the neutrino mass matrix are given while the charged lepton mass matrix has off-diagonal components.[1] Then, zeros of the neutrino mass matrix are polluted after diagonalizing the charged lepton mass matrix. Therefore we need to study the stability of predictions of the texture zeros by taking account of small corrections to zeros.

[1] There are some models in which zeros of the neutrino mass matrix are realized in the diagonal basis of the charged lepton mass matrix [15]–[17].

In this paper, we present detailed study of the neutrino mixing parameter U_{e3} and CP violating quantity J_{CP} [18], which are expected to be affected by the small corrections to zeros in the neutrino mass matrix. It is found that the predicted U_{e3} and J_{CP} considerably depend on these corrections.

Predictions of the texture two zeros are presented in section 2. Small corrections to zeros are discussed and the stability of predictions are studied in section 3. Section 4 is devoted to the summary.

2. Predictions of texture two zeros

There are 15 textures with two zeros for the effective neutrino mass matrix M_ν, which have five independent parameters. The two zero conditions give

$$(M_\nu)_{ab} = \sum_{i=1}^{3} U_{ai} U_{bi} \lambda_i = 0\,, \qquad (M_\nu)_{\alpha\beta} = \sum_{i=1}^{3} U_{\alpha i} U_{\beta i} \lambda_i = 0\,, \tag{2.1}$$

where λ_i is the i-th eigenvalue including the Majorana phases, and indices (ab) and $(\alpha\beta)$ denote the flavor components, respectively.

Solving these equations, ratios of neutrino masses m_1, m_2, m_3, which are absolute values of λ_i's, are given in terms of the neutrino mixing matrix U [19] as follows:

$$\begin{aligned} \frac{m_1}{m_3} &= \left| \frac{U_{a3}U_{b3}U_{\alpha 2}U_{\beta 2} - U_{a2}U_{b2}U_{\alpha 3}U_{\beta 3}}{U_{a2}U_{b2}U_{\alpha 1}U_{\beta 1} - U_{a1}U_{b1}U_{\alpha 2}U_{\beta 2}} \right| , \\ \frac{m_2}{m_3} &= \left| \frac{U_{a1}U_{b1}U_{\alpha 3}U_{\beta 3} - U_{a3}U_{b3}U_{\alpha 1}U_{\beta 1}}{U_{a2}U_{b2}U_{\alpha 1}U_{\beta 1} - U_{a1}U_{b1}U_{\alpha 2}U_{\beta 2}} \right| . \end{aligned} \tag{2.2}$$

Then, one can test textures in the ratio R_ν,

$$R_\nu \equiv \left| \frac{m_2^2 - m_1^2}{m_3^2 - m_2^2} \right| \approx \frac{\Delta m^2_{\rm sun}}{\Delta m^2_{\rm atm}}\,, \tag{2.3}$$

which has been given by the experimental data. The ratio R_ν is given only in terms of four parameters (three mixing angles and one phase) in

$$U = \begin{pmatrix} c_{13}c_{12} & c_{13}s_{12} & s_{13}e^{-i\delta} \\ -c_{23}s_{12} - s_{23}s_{13}c_{12}e^{i\delta} & c_{23}c_{12} - s_{23}s_{13}s_{12}e^{i\delta} & s_{23}c_{13} \\ s_{23}s_{12} - c_{23}s_{13}c_{12}e^{i\delta} & -s_{23}c_{12} - c_{23}s_{13}s_{12}e^{i\delta} & c_{23}c_{13} \end{pmatrix}, \tag{2.4}$$

where c_{ij} and s_{ij} denote $\cos\theta_{ij}$ and $\sin\theta_{ij}$, respectively.

Seven acceptable textures with two independent zeros were found for the neutrino mass matrix [10], and they have been studied in detail [12, 13].[2] Among them, the textures A_1 and A_2 of ref. [10], which correspond to the hierarchical neutrino mass spectrum, are strongly favored by the recent phenomenological analyses [11]–[13]. Therefore, we study these two textures in this paper.

[2] Additional two textures may be allowed marginally by current data as shown in ref. [12].

In the texture A_1, which has two zeros as $(M_\nu)_{ee} = 0$ and $(M_\nu)_{e\mu} = 0$, the mass ratios are given as

$$\begin{aligned}\frac{m_1}{m_3} &= \left|\frac{s_{13}}{c_{13}^2}\left(\frac{s_{12}s_{23}}{c_{12}c_{23}} - s_{13}e^{-i\delta}\right)\right|, \\ \frac{m_2}{m_3} &= \left|\frac{s_{13}}{c_{13}^2}\left(\frac{c_{12}s_{23}}{s_{12}c_{23}} + s_{13}e^{-i\delta}\right)\right|.\end{aligned} \tag{2.5}$$

In the texture A_2, which has two zeros as $(M_\nu)_{ee} = 0$ and $(M_\nu)_{e\tau} = 0$, the mass ratios are given as

$$\begin{aligned}\frac{m_1}{m_3} &= \left|\frac{s_{13}}{c_{13}^2}\left(\frac{s_{12}c_{23}}{c_{12}s_{23}} + s_{13}e^{-i\delta}\right)\right|, \\ \frac{m_2}{m_3} &= \left|\frac{s_{13}}{c_{13}^2}\left(\frac{c_{12}c_{23}}{s_{12}s_{23}} - s_{13}e^{-i\delta}\right)\right|.\end{aligned} \tag{2.6}$$

It is remarked that the mass ratios of the texture A_2 are given exactly by replacing $\tan\theta_{23}$ in A_1 with $-\cot\theta_{23}$.

If θ_{12}, θ_{23}, θ_{13} and δ are fixed, we can predict R_ν of eq. (2.3), which is compared with the experimental value $\Delta m^2_{\rm sun}/\Delta m^2_{\rm atm}$. Taking account of the following data with 90% C.L. [5],

$$\begin{aligned}\sin^2 2\theta_{\rm atm} &\geq 0.92\,, & \Delta m^2_{\rm atm} &= (1.5 \sim 3.9) \times 10^{-3}\,{\rm eV}^2\,, \\ \tan^2\theta_{\rm sun} &= 0.33 \sim 0.67\,, & \Delta m^2_{\rm sun} &= (6 \sim 8.5) \times 10^{-5}\,{\rm eV}^2\,,\end{aligned} \tag{2.7}$$

with $\sin\theta_{\rm CHOOZ} \leq 0.2$, we predict R_ν. In figure 1, we present the scatter plot of the predicted R_ν versus $\sin\theta_{13}$, in which δ is taken in the whole range $-\pi \sim \pi$ for the texture A_1. The parameters are taken in the following ranges of $\theta_{12} = 30^\circ \sim 39^\circ$, $\theta_{23} = 37^\circ \sim 53^\circ$, $\theta_{13} = 1^\circ \sim 12^\circ$ and $\delta = -\pi \sim \pi$. It is found that many predicted values of R_ν lie outside the experimental allowed region. This result means that there is a strong constraint for the parameter θ_{13}. We get $\sin\theta_{13} \geq 0.05$ from the experimental value of R_ν as seen in figure 1.

In order to present the allowed region of $\sin\theta_{13}$ for the texture A_1, we show the scatter plot of $\sin\theta_{13}$ versus $\tan^2\theta_{12}$ and $\tan^2\theta_{23}$ in figure 2 and figure 3, respectively. If we take the best fit values of $\tan^2\theta_{12} = 0.42$, $\tan^2\theta_{23} = 1$, $\Delta m^2_{\rm sun} = 7.3 \times 10^{-5}\,{\rm eV}^2$ and $\Delta m^2_{\rm atm} = 2.5 \times 10^{-3}\,{\rm eV}^2$, the prediction of $\sin\theta_{13}$ is $0.11 \sim 0.14$, where the phase δ is taken in the whole range $-\pi \sim \pi$. In figure 4, we show J_{CP} versus $\sin\theta_{13}$ for the texture A_1. Since J_{CP} is proportional to $\sin\theta_{13}$ and $\sin\delta$, we also show the allowed region of δ versus $\sin\theta_{13}$ in figure 5. It is found that δ is allowed in the whole range of $-\pi \sim \pi$.

We do not show the numerical results in the texture A_2 because those are obtained only by replacing $\tan\theta_{23}$ in A_1 with $-\cot\theta_{23}$.

The allowed regions in figure 2 and figure 3 are quantitatively understandable in the following approximate relations:

$$|U_{e3}| \equiv \sin\theta_{13} \simeq \frac{1}{2}\tan 2\theta_{12}\ \cot\theta_{23}\sqrt{R_\nu\cos 2\theta_{12}}\,, \tag{2.8}$$

for the texture A_1, and

$$|U_{e3}| \equiv \sin\theta_{13} \simeq \frac{1}{2}\tan 2\theta_{12}\ \tan\theta_{23}\sqrt{R_\nu\cos 2\theta_{12}}\,, \tag{2.9}$$

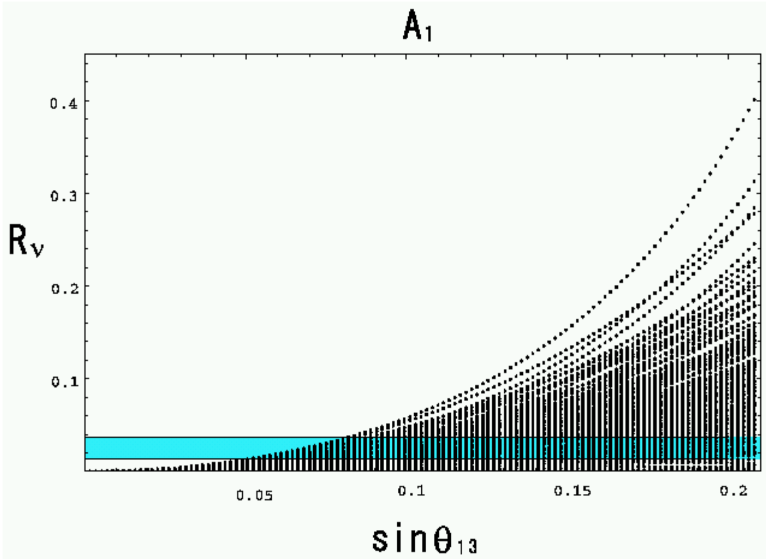

Figure 1: Scatter plot of R_ν versus $\sin\theta_{13}$ for A_1. The unknown phase δ is taken in the whole range $-\pi \sim \pi$. The gray horizontal band is the experimental allowed region.

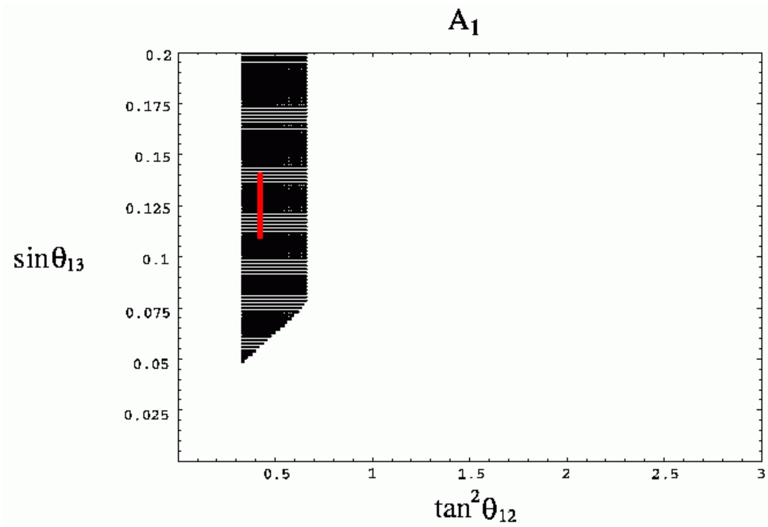

Figure 2: Scatter plot of $\sin\theta_{13}$ versus $\tan^2\theta_{12}$ for A_1. The best fit is shown by a red line.

for the texture A_2, respectively, where the phase δ is neglected because it is a next leading term. As $\tan\theta_{12}$ increases, the lower bound of $|U_{e3}|$ increases, and as $\tan\theta_{23}$ decreases, it increases. It is found in figure 2 that the lower bound $|U_{e3}| = 0.05$ is given in the case of the smallest $\tan^2\theta_{12}$, while $|U_{e3}| = 0.08$ is given in the largest $\tan^2\theta_{12}$. On the other hand, as seen in figure 3, the lower bound $|U_{e3}| = 0.05$ is given in the largest $\tan^2\theta_{23}$, while $|U_{e3}| = 0.08$ is given in the smallest $\tan^2\theta_{23}$. The upper bound of $|J_{CP}|$ is 0.05, but $J_{CP} = 0$ is still allowed in figure 4. These predicted regions will be reduced in the future since error bars of experimental data in eq. (2.7) will be reduced, especially, KamLAND is expected to determine Δm^2_{12} precisely.

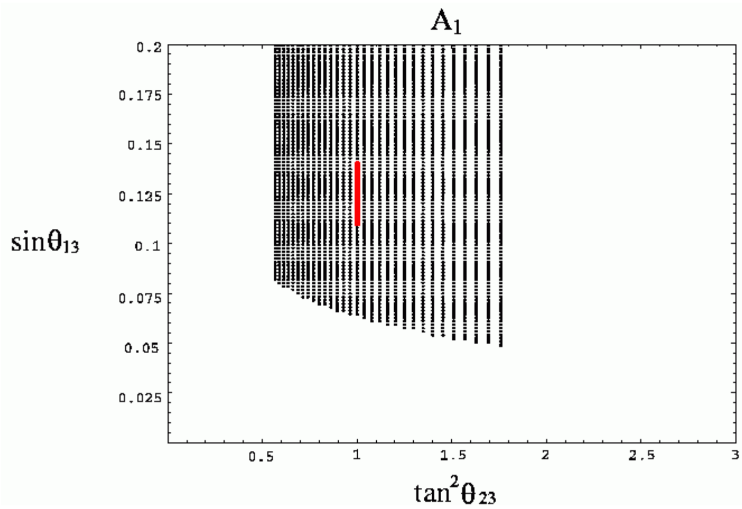

Figure 3: Scatter plot of $\sin\theta_{13}$ versus $\tan^2\theta_{23}$ for A_1. The best fit is shown by a red line.

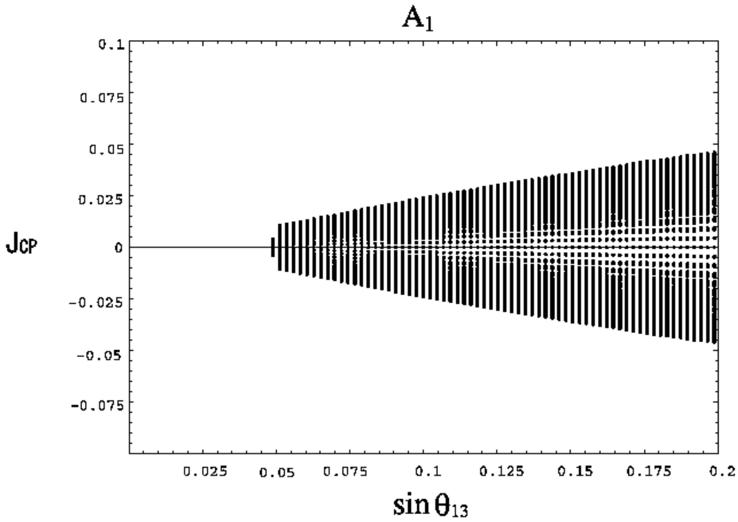

Figure 4: Scatter plot of J_{CP} versus $\sin\theta_{13}$ for A_1.

3. Stability of predicted U_{e3}

Above predictions are important ones in the texture zeros. The relative magnitude of each entry of the neutrino mass matrix is roughly given as follows:

$$M_\nu \sim \begin{pmatrix} 0 & 0 & \lambda \\ 0 & 1 & 1 \\ \lambda & 1 & 1 \end{pmatrix} \quad \text{for } A_1\,, \qquad \begin{pmatrix} 0 & \lambda & 0 \\ \lambda & 1 & 1 \\ 0 & 1 & 1 \end{pmatrix} \quad \text{for } A_2\,, \tag{3.1}$$

where $\lambda \simeq 0.2$. However, these texture zeros are not preserved to all orders. Even if zero-entries of the mass matrix are given at the high energy scale, non-zero components may evolve instead of zeros at the low energy scale due to radiative corrections. Those magnitudes depend on unspecified interactions from which lepton masses are generated.

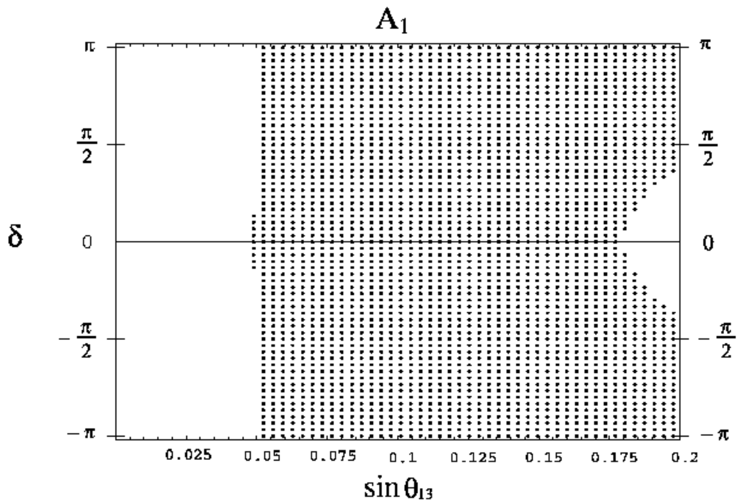

Figure 5: Scatter plot of δ versus $\sin\theta_{13}$ for A_1.

Moreover, zeros of the neutrino mass matrix are given while the charged lepton mass matrix has off-diagonal components in the model with some flavor symmetry. Then, zeros are not realized in the diagonal basis of the charged lepton mass matrix. In other words, zeros of the neutrino mass matrix is polluted by the small off-diagonal elements of the charged lepton mass matrix.

Therefore, one need the careful study of stability of the prediction for $|U_{e3}|$ and J_{CP} because these are small quantities. In order to see the effect of the small non-zero components, the conditions of zeros in eq. (2.1) are modified. The two conditions turn to

$$(M_\nu)_{ab} = \sum_{i=1}^{3} U_{ai}U_{bi}\lambda_i = \epsilon\,, \qquad (M_\nu)_{\alpha\beta} = \sum_{i=1}^{3} U_{\alpha i}U_{\beta i}\lambda_i = \omega\,, \tag{3.2}$$

where ϵ and ω are arbitrary parameters with the mass unit, which are much smaller than other non-zero components of the mass matrix. These parameters are supposed to be real for simplicity. We get

$$\begin{aligned}\frac{m_1}{m_3} &= \left|\frac{U_{13}U_{13}U_{12}U_{22} - U_{12}U_{12}U_{13}U_{23} - U_{12}U_{22}\overline{\epsilon} + U_{12}U_{12}\overline{\omega}}{U_{12}U_{12}U_{11}U_{21} - U_{11}U_{11}U_{12}U_{22}}\right|,\\ \frac{m_2}{m_3} &= \left|\frac{U_{11}U_{11}U_{13}U_{23} - U_{13}U_{13}U_{11}U_{21} + U_{11}U_{21}\overline{\epsilon} - U_{11}U_{11}\overline{\omega}}{U_{12}U_{12}U_{11}U_{21} - U_{11}U_{11}U_{12}U_{22}}\right|,\end{aligned} \tag{3.3}$$

for the texture A_1, and

$$\begin{aligned}\frac{m_1}{m_3} &= \left|\frac{U_{13}U_{13}U_{12}U_{32} - U_{12}U_{12}U_{13}U_{33} - U_{12}U_{32}\overline{\epsilon} + U_{12}U_{12}\overline{\omega}}{U_{12}U_{12}U_{11}U_{31} - U_{11}U_{11}U_{12}U_{32}}\right|,\\ \frac{m_2}{m_3} &= \left|\frac{U_{11}U_{11}U_{13}U_{33} - U_{13}U_{13}U_{11}U_{31} + U_{11}U_{31}\overline{\epsilon} - U_{11}U_{11}\overline{\omega}}{U_{12}U_{12}U_{11}U_{31} - U_{11}U_{11}U_{12}U_{32}}\right|,\end{aligned} \tag{3.4}$$

for the texture A_2, where $\bar{\epsilon}$ and $\bar{\varpi}$ are normalized ones as $\bar{\epsilon} = \epsilon/\lambda_3$ and $\bar{\varpi} = \omega/\lambda_3$, respectively. We obtain approximately

$$\begin{aligned}\frac{m_1}{m_3} &\simeq \left| t_{12} t_{23} s_{13} e^{-i\delta} - \frac{t_{12}}{c_{23}} \bar{\varpi} + \bar{\epsilon} \right| , \\ \frac{m_2}{m_3} &\simeq \left| \frac{1}{t_{12}} t_{23} s_{13} e^{-i\delta} - \frac{1}{t_{12} c_{23}} \bar{\varpi} - \bar{\epsilon} \right| ,\end{aligned} \tag{3.5}$$

for the texture A_1, and

$$\begin{aligned}\frac{m_1}{m_3} &\simeq \left| -t_{12} \frac{1}{t_{23}} s_{13} e^{-i\delta} + \frac{t_{12}}{s_{23}} \bar{\varpi} + \bar{\epsilon} \right| , \\ \frac{m_2}{m_3} &\simeq \left| -\frac{1}{t_{12} t_{23}} s_{13} e^{-i\delta} + \frac{1}{t_{12} s_{23}} \bar{\varpi} - \bar{\epsilon} \right| ,\end{aligned} \tag{3.6}$$

for the texture A_2, where $t_{ij} = \tan\theta_{ij}$. We present the approximate expression of $|U_{e3}| = \sin\theta_{13}$ as follows:

$$\sin\theta_{13} \simeq \pm\frac{1}{2} \tan 2\theta_{12} \ \cot\theta_{23} \sqrt{R_\nu \cos 2\theta_{12}} + \frac{\bar{\varpi} \ \cos\delta}{s_{23}} + \frac{t_{12}}{t_{23}} \frac{\bar{\epsilon} \ \cos\delta}{1 - t_{12}^2} + O(\bar{\varpi}^2, \ \bar{\epsilon}^2) \, , \tag{3.7}$$

for the texture A_1, and

$$\sin\theta_{13} \simeq \pm\frac{1}{2} \tan 2\theta_{12} \ \tan\theta_{23} \sqrt{R_\nu \cos 2\theta_{12}} + \frac{\bar{\varpi} \ \cos\delta}{c_{23}} - t_{12} t_{23} \frac{\bar{\epsilon} \ \cos\delta}{1 - t_{12}^2} + O(\bar{\varpi}^2, \ \bar{\epsilon}^2) \, , \tag{3.8}$$

for the texture A_2. In these equations, $+(-)$ of the first term in the right-hand side corresponds to the case of $\tan\theta_{12} \tan\theta_{23} > 0 (< 0)$. It is remarked that the second and third terms in the right-hand side could be comparable with the first one in eq. (3.7) and eq. (3.8).

However, the second and third terms in the right-hand side could be partially canceled each other depending on the sign of $\tan\theta_{12}$ and $\tan\theta_{23}$. Therefore, the prediction of $|U_{e3}|$ is somewhat different between the texture A_1 and A_2.

In order to estimate the effect of $\bar{\varpi}$ and $\bar{\epsilon}$, we consider the case in which the charged lepton mass matrix has small off-diagonal components. Suppose that the two zeros in eq. (3.1) is still preserved for the neutrino sector. The typical model of the charged lepton is the Georgi-Jarlskog texture [20], in which the charged lepton mass matrix M_E is given as

$$M_E \simeq \begin{pmatrix} 0 & \sqrt{m_e m_\mu} & 0 \\ \sqrt{m_e m_\mu} & m_\mu & \sqrt{m_e m_\tau} \\ 0 & \sqrt{m_e m_\tau} & m_\tau \end{pmatrix} , \tag{3.9}$$

where each matrix element is written in terms of the charged lepton masses, and phases are neglected for simplicity. This matrix is diagonalized by the unitary matrix U_E, in which the mixing between the first and second families is $\sqrt{m_e/m_\mu} \simeq 0.07$ and the mixing between the second and third families is $\sqrt{m_e/m_\tau} \simeq 0.02$. Since the neutrino mass matrix is still

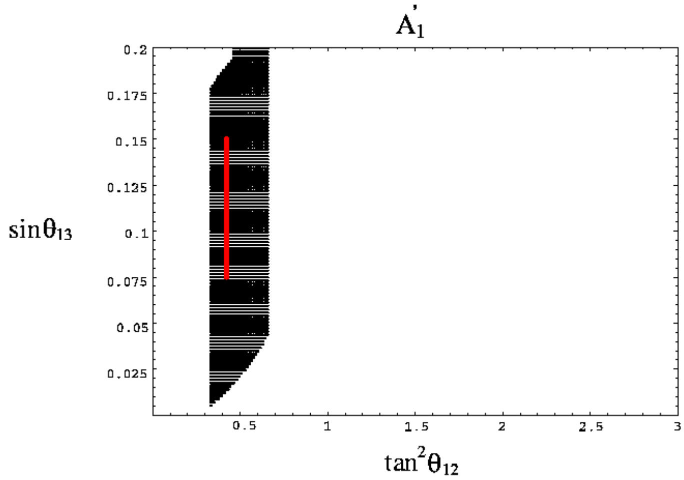

Figure 6: Scatter plot of $\sin\theta_{13}$ versus $\tan^2\theta_{12}$ in the case of $\kappa = 2\overline{\omega} = 0.07$ for A_1'. The best fit is shown by a red line.

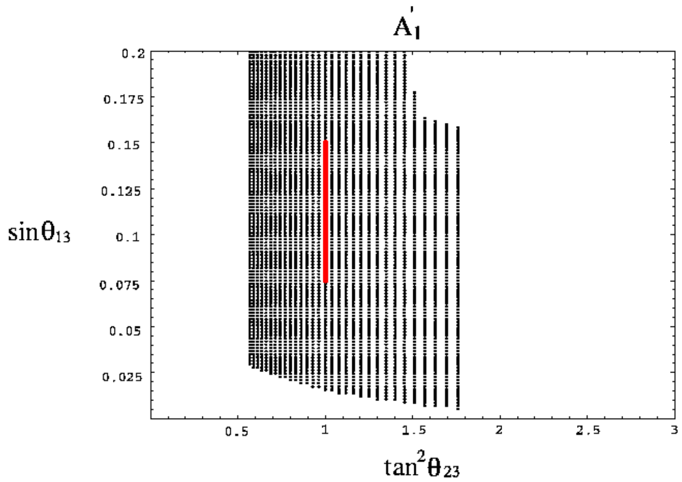

Figure 7: Scatter plot of $\sin\theta_{13}$ versus $\tan^2\theta_{23}$ in the case of $\kappa = 2\overline{\omega} = 0.07$ for A_1'. The best fit is shown by a red line.

the texture A_1 or the texture A_2,[3] it turns to A_1' or A_2' as follows:

$$M_\nu \sim \begin{pmatrix} \kappa^2 & \kappa & \lambda \\ \kappa & 1 & 1 \\ \lambda & 1 & 1 \end{pmatrix} \quad \text{for } A_1', \qquad \begin{pmatrix} 2\kappa\lambda & \lambda & \kappa \\ \lambda & 1 & 1 \\ \kappa & 1 & 1 \end{pmatrix} \quad \text{for } A_2', \tag{3.10}$$

in the diagonal basis of the charged lepton mass matrix. Therefore, the parameter $\overline{\epsilon}$ are correlated with $\overline{\omega}$ such as $\overline{\omega} \simeq \kappa/2$ and $\overline{\epsilon} \simeq \kappa^2/2$ in the texture A_1', and $\overline{\omega} \simeq \kappa/2$ and $\overline{\epsilon} \simeq \kappa\lambda$ in the texture A_2'.

By using the texture A_1' of the neutrinos in eq. (3.10), we show our results of the allowed region of $\sin\theta_{13}$ versus $\tan^2\theta_{12}$ and $\tan^2\theta_{23}$ in figure 6 and figure 7, respectively, where $\tan\theta_{12}$ and $\tan\theta_{23}$ are taken to be positive. In the case of the best fit values of

[3]The combined model with Georgi-Jarlskog texture and the A_2 type one is presented in ref. [14]

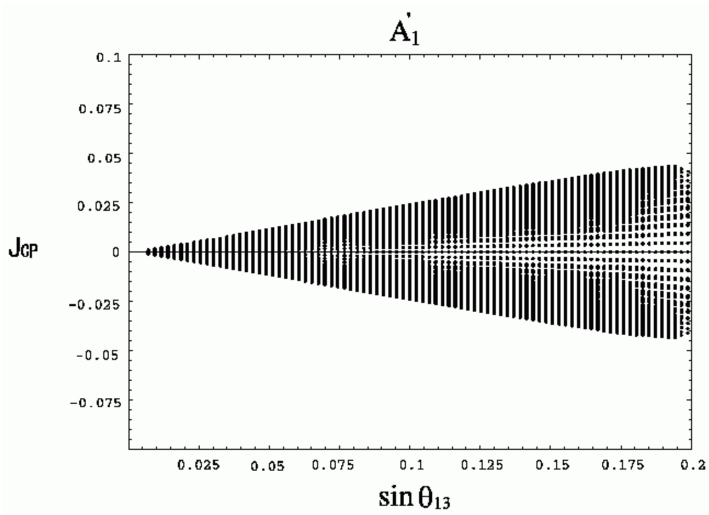

Figure 8: Scatter plot of J_{CP} versus $\sin\theta_{13}$ in the case of $\kappa = 2\overline{\omega} = 0.07$ for A_1'.

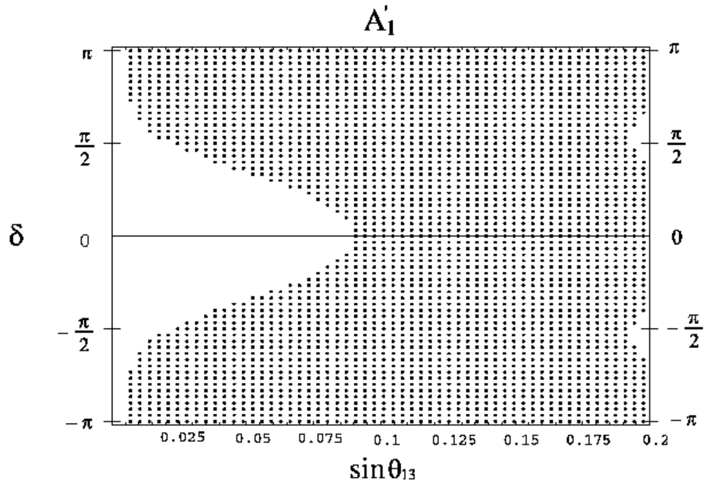

Figure 9: Scatter plot of δ versus $\sin\theta_{13}$ for A_1'.

$\tan^2\theta_{12}$, $\tan^2\theta_{23}$, $\Delta m^2_{\rm sun}$ and $\Delta m^2_{\rm atm}$, the prediction of $\sin\theta_{13}$ is $0.075 \sim 0.15$, which is somewhat wider than the result of the section 2 due to the correction κ. We have also calculated in the case of $\tan\theta_{12}\tan\theta_{23} < 0$. Predictions are almost same because of $\overline{\omega} \gg \overline{\epsilon}$. In figure 8, we show J_{CP} versus $\sin\theta_{13}$. We also show the allowed region of δ versus $\sin\theta_{13}$ in figure 9. These results should be compared with the ones in figure 2 $\sim$ figure 5. It is noticed that the lower bound of $\sin\theta_{13}$ considerably comes down due to the correction κ. The small $|U_{e3}|$ of 8×10^{-3} is allowed. In figure 6 and figure 7, we also find that there is an upper bound on $|U_{e3}|$ for small values of $\tan^2\theta_{12}$ and large values of $\tan^2\theta_{23}$. We have checked numerically that this upper bound appears due to the higher order terms, which are omitted in eqs. (3.5), (3.6) and (3.7) and (3.8). As seen in figure 9, the phase δ is not allowed in the whole range $-\pi \sim \pi$ if $\sin\theta_{12} \leq 0.09$.

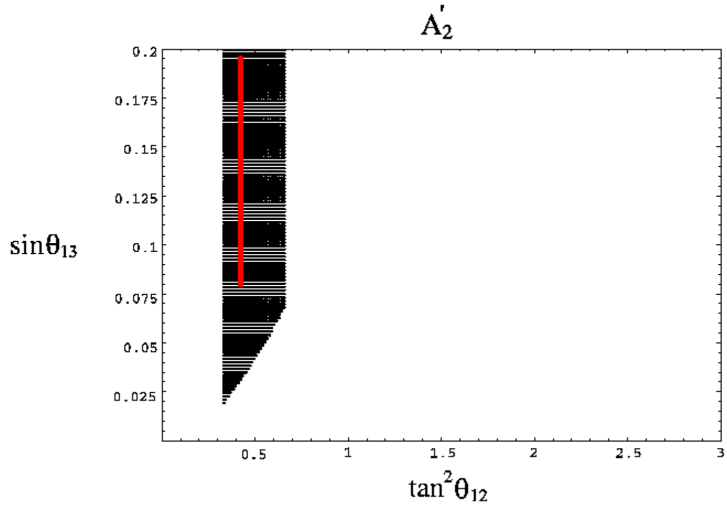

Figure 10: Scatter plot of $\sin\theta_{13}$ versus $\tan^2\theta_{12}$ in the case of $\kappa = 2\overline{\omega} = 0.07$ for A'_2. The best fit is shown by a red line.

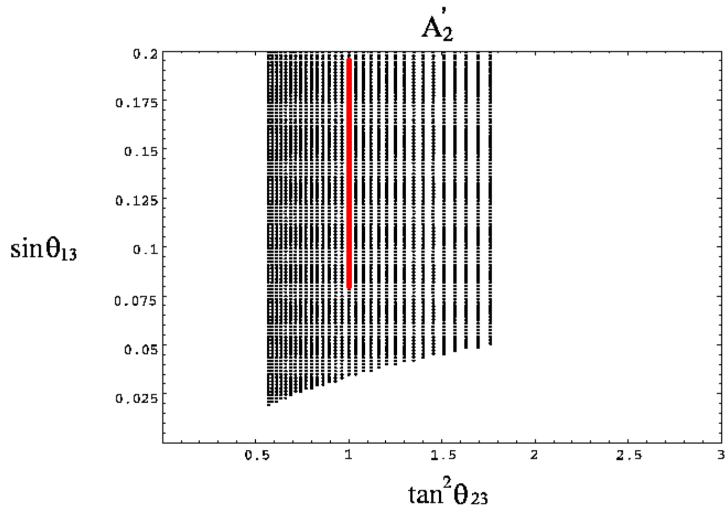

Figure 11: Scatter plot of $\sin\theta_{13}$ versus $\tan^2\theta_{12}$ in the case of $\kappa = 2\overline{\omega} = 0.07$ for A'_2. The best fit is shown by a red line.

In the texture A'_2 of eq. (3.10), we show allowed regions of $\sin\theta_{13}$ versus $\tan^2\theta_{12}$ and $\tan^2\theta_{23}$ in figure 10 and figure 11, respectively. In the case of the best fit values of $\tan^2\theta_{12}$, $\tan^2\theta_{23}$, $\Delta m^2_{\rm sun}$ and $\Delta m^2_{\rm atm}$, the prediction of $\sin\theta_{13}$ is $0.08 \sim 0.195$, which is somewhat different from the result of A'_1. There is no upper bound on $|U_{e3}|$ in figure 10 and figure 11. The effect of $\overline{\omega}$ is canceled partially by the effect of $\overline{\epsilon}$ as seen in eq. (3.8). Therefore, allowed regions in figure 10 and figure 11 are somewhat different from ones in figure 6 and figure 7. We show the result in the case of $\tan\theta_{12}\tan\theta_{23} < 0$ in figure 12 and figure 13. The lower bound of $\sin\theta_{13}$ comes down to zero, which is contrasted with the result in figure 10 and figure 11 because there is no cancellation between the effect of $\overline{\omega}$ and $\overline{\epsilon}$ as seen in eq. (3.8). We omit the figure of J_{CP} because it is almost same as the result in the case of A'_1.

JHEP09(2003)028

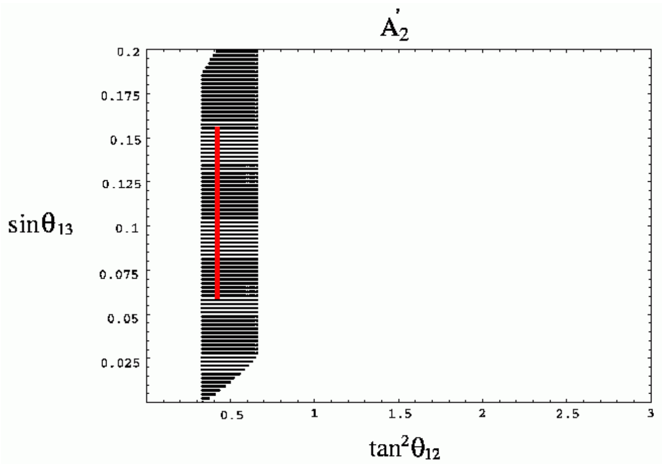

Figure 12: Scatter plot of $\sin\theta_{13}$ versus $\tan^2\theta_{23}$ in the case of $\tan\theta_{12}\tan\theta_{23} < 0$ with $\kappa = 2\overline{\omega} = 0.07$ for A_2'. The best fit is shown by a red line.

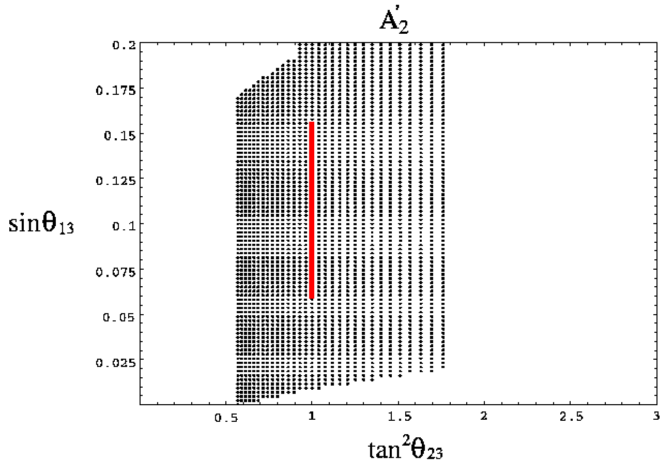

Figure 13: Scatter plot of $\sin\theta_{13}$ versus $\tan^2\theta_{23}$ in the case of $\tan\theta_{12}\tan\theta_{23} < 0$ with $\kappa = 2\overline{\omega} = 0.07$ for A_2'. The best fit is shown by a red line.

This result depends on a specific model. In order to complete the study of the stability, we also consider the case that two corrections $\overline{\epsilon}$ and $\overline{\omega}$ are independent each other, which may be the case if the deviation from zero arises from radiative corrections. For the texture A_1', we show the allowed region of $\sin\theta_{13}$ versus $2\overline{\omega}$ in figure 14, where $\overline{\epsilon} = 0$ is taken. The gray region is allowed by the experimental data for the texture A_1'. The allowed region of the texture A_2' is almost same as the one of A_1'. In figure 14, the narrow deep gray region is only added in the case of the texture A_2'. We also show the allowed region of $\sin\theta_{13}$ versus $\overline{\epsilon}$ in figure 15, in which $\overline{\omega} = 0$ is taken. There is no difference between the allowed region of both A_1' and A_2'.

The predicted lower bound of $|U_{e3}|$ is sensitive to $\overline{\omega}$. If the correction $\overline{\omega}$ is as large as 0.02, the lower bound of $|U_{e3}|$ comes down to 0.025. If $\overline{\omega}$ is larger than 0.04, the predictability of $|U_{e3}|$ is lost since $|U_{e3}| = 0$ is allowed. On the other hand, the lower bound

JHEP09(2003)028

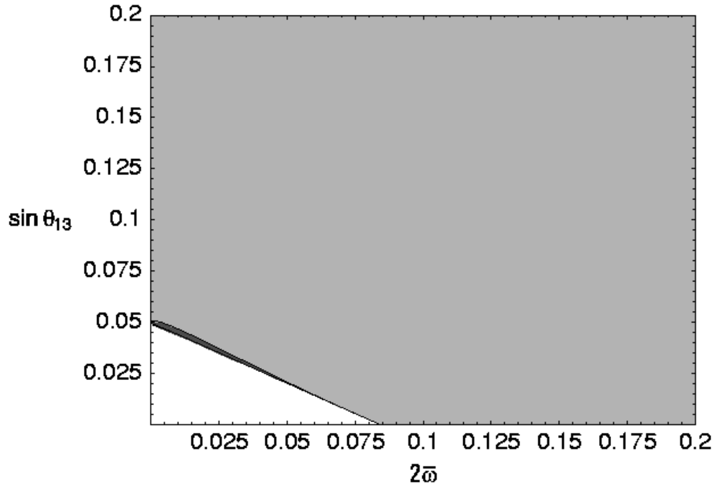

Figure 14: Prediction of $\sin\theta_{13}$ versus $2\overline{\varpi}$ in the case of $\overline{\epsilon} = 0$. The gray region is allowed by the experimental data for A_1'. The deep gray region is added for A_2'.

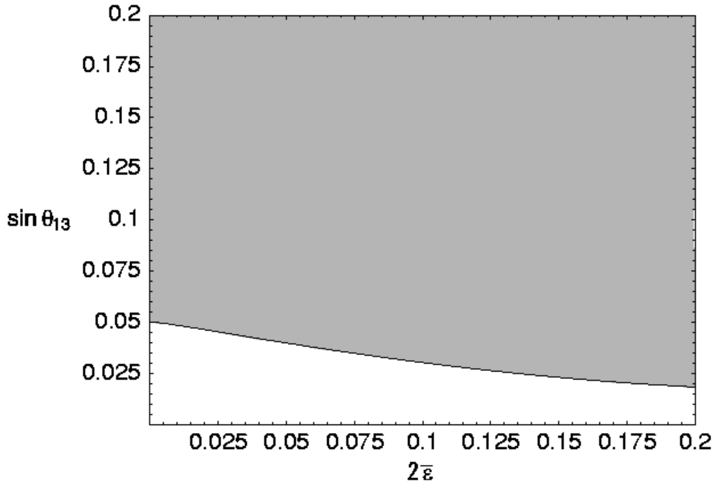

Figure 15: Prediction of $\sin\theta_{13}$ versus $2\overline{\epsilon}$ in the case of $\overline{\varpi} = 0$ for both A_1' and A_2'. The gray region is allowed by the experimental data.

is rather insensitive to $\overline{\epsilon}$. Even if the correction $\overline{\epsilon}$ grows up to be 0.1, the lower bound of $|U_{e3}|$ is still 0.02. It is concluded that the magnitude of the deviation from the zero in the $(1,2)/(1,3)$ element for the texture A_1/A_2 is important to predict $|U_{e3}|$.

4. Summary

We summarize our results as follows. We have studied $|U_{e3}|$ and J_{CP} in the textures A_1 and A_2 of the neutrino mass matrix with two zeros. The lower bound of $|U_{e3}|$ is 0.05, which considerably depends on $\tan^2\theta_{12}$ and $\tan^2\theta_{23}$. We have investigated the stability of these predictions by taking account of small corrections, which may come from radiative corrections or off-diagonal elements of the charged lepton mass matrix. The lower bound of

$|U_{e3}|$ comes down significantly in the case of $\overline{\varpi} \gg 0.01$, while $\overline{\epsilon}$ is rather insensitive to $|U_{e3}|$. Therefore the corrections to the texture zeros in the (1,2)/(1,3) element for the texture A_1/A_2 should be carefully taken to predict $|U_{e3}|$.

In the case of best fit values of $\tan^2\theta_{12}$, $\tan^2\theta_{23}$, $\Delta m^2_{\rm sun}$ and $\Delta m^2_{\rm atm}$, the prediction of $|U_{e3}|$ is $0.075 \sim 0.195$ even if the corrections are taken into account. This prediction is good news for the near future experiments. The measurement of $|U_{e3}|$ will be an important test of the texture zeros in the future.

Acknowledgments

We would like to thank M. Katsumata, H. Nakano and H. So for helpful discussions. We are also grateful to KITP in UCSB, where the paper was completed, for its warm hospitality. This research was supported in part by the National Science Foundation in USA under Grant No. PHY99-07949 and the Grant-in-Aid for Science Research, Ministry of Education, Science and Culture, Japan(No.12047220).

References

[1] Super-Kamiokande collaboration, Y. Fukuda et al., *Evidence for oscillation of atmospheric neutrinos*, *Phys. Rev. Lett.* **81** (1998) 1562 [hep-ex/9807003]; *Measurement of the flux and zenith-angle distribution of upward through-going muons by super-Kamiokande*, *Phys. Rev. Lett.* **82** (1999) 2644 [hep-ex/9812014];
Super-Kamiokande collaboration, T. Futagami et al., *Observation of the east-west anisotropy of the atmospheric neutrino flux*, *Phys. Rev. Lett.* **82** (1999) 5194 [astro-ph/9901139].

[2] Super-Kamiokande collaboration, S. Fukuda et al., *Solar* ^{8}B *and* He *p neutrino measurements from 1258 days of super-Kamiokande data*, *Phys. Rev. Lett.* **86** (2001) 5651 [hep-ex/0103032].

[3] SNO collaboration, Q.R. Ahmad et al., *Measurement of the charged current interactions produced by* ^{8}B *solar neutrinos at the sudbury neutrino observatory*, *Phys. Rev. Lett.* **87** (2001) 071301 [nucl-ex/0106015]; *Direct evidence for neutrino flavor transformation from neutral-current interactions in the sudbury neutrino observatory*, *Phys. Rev. Lett.* **89** (2002) 011301 [nucl-ex/0204008]; *Measurement of day and night neutrino energy spectra at sno and constraints on neutrino mixing parameters*, *Phys. Rev. Lett.* **89** (2002) 011302 [nucl-ex/0204009].

[4] KamLAND collaboration, K. Eguchi et al., *First results from KamLAND: evidence for reactor anti-neutrino disappearance*, *Phys. Rev. Lett.* **90** (2003) 021802 [hep-ex/0212021].

[5] G.L. Fogli, E. Lisi, M. Marrone, D. Montanino, A. Palazzo and A.M. Rotunno, *Solar neutrino oscillation parameters after first KamLAND results*, *Phys. Rev.* **D 67** (2003) 073002 [hep-ph/0212127];
J.N. Bahcall, M.C. Gonzalez-Garcia and C. Pena-Garay, *Solar neutrinos before and after KamLAND*, *J. High Energy Phys.* **02** (2003) 009 [hep-ph/0212147];
M. Maltoni, T. Schwetz and J.W.F. Valle, *Combining first KamLAND results with solar neutrino data*, *Phys. Rev.* **D 67** (2003) 093003 [hep-ph/0212129];

P.C. de Holanda and A.Y. Smirnov, *Lma msw solution of the solar neutrino problem and first KamLAND results*, *JCAP* **0302** (2003) 001 [hep-ph/0212270];
V. Barger and D. Marfatia, *KamLAND and solar neutrino data eliminate the low solution*, *Phys. Lett.* **B 555** (2003) 144 [hep-ph/0212126].

[6] CHOOZ collaboration, M. Apollonio et al., *Limits on neutrino oscillations from the CHOOZ experiment*, *Phys. Lett.* **B 466** (1999) 415 [hep-ex/9907037].

[7] H. Nishiura, K. Matsuda and T. Fukuyama, *Lepton and quark mass matrices*, *Phys. Rev.* **D 60** (1999) 013006 [hep-ph/9902385].

[8] E.K. Akhmedov, G.C. Branco and M.N. Rebelo, *Linking solar and long baseline terrestrial neutrino experiments*, *Phys. Rev. Lett.* **84** (2000) 3535 [hep-ph/9912205].

[9] S.K. Kang and C.S. Kim, *Majorana neutrino masses and neutrino oscillations*, *Phys. Rev.* **D 63** (2001) 113010 [hep-ph/0012046].

[10] P.H. Frampton, S.L. Glashow and D. Marfatia, *Zeroes of the neutrino mass matrix*, *Phys. Lett.* **B 536** (2002) 79 [hep-ph/0201008].

[11] Z. Xing, *Texture zeros and majorana phases of the neutrino mass matrix*, *Phys. Lett.* **B 530** (2002) 159 [hep-ph/0201151].

[12] W. Guo and Z.-z. Xing, *Implications of the KamLAND measurement on the lepton flavor mixing matrix and the neutrino mass matrix*, *Phys. Rev.* **D 67** (2003) 053002 [hep-ph/0212142].

[13] R. Barbieri, T. Hambye and A. Romanino, *Natural relations among physical observables in the neutrino mass matrix*, *J. High Energy Phys.* **03** (2003) 017 [hep-ph/0302118].

[14] M. Bando and M. Obara, *Neutrino mass matrix out of up-quark masses only*, hep-ph/0212242.

[15] A. Zee, *A theory of lepton number violation, neutrino majorana mass and oscillation*, *Phys. Lett.* **B 93** (1980) 389; *Charged scalar field and quantum number violations*, *Phys. Lett.* **B 161** (1985) 141;
L. Wolfenstein, *A theoretical pattern for neutrino oscillations*, *Nucl. Phys.* **B 175** (1980) 93;
S.T. Petcov, *Remarks on the zee model of neutrino mixing ($\mu \to e\gamma$, heavy neutrino $\to$ light neutrino gamma, etc.)*, *Phys. Lett.* **B 115** (1982) 401;
C. Jarlskog, M. Matsuda, S. Skadhauge and M. Tanimoto, *Zee mass matrix and bimaximal neutrino mixing*, *Phys. Lett.* **B 449** (1999) 240 [hep-ph/9812282];
P.H. Frampton and S.L. Glashow, *Can the Zee ansatz for neutrino masses be correct?*, *Phys. Lett.* **B 461** (1999) 95 [hep-ph/9906375].

[16] P.H. Frampton, M.C. Oh and T. Yoshikawa, *Majorana mass zeroes from triplet vev without Majoron problem*, *Phys. Rev.* **D 66** (2002) 033007 [hep-ph/0204273].

[17] A. Kageyama, S. Kaneko, N. Shimoyama and M. Tanimoto, *Seesaw realization of the texture zeros in the neutrino mass matrix*, *Phys. Lett.* **B 538** (2002) 96 [hep-ph/0204291].

[18] C. Jarlskog, *Commutator of the quark mass matrices in the standard electroweak model and a measure of maximal CP-violation*, *Phys. Rev. Lett.* **55** (1985) 1039.

[19] Z. Maki, M. Nakagawa and S. Sakata, *Remarks on the unified model of elementary particles*, *Prog. Theor. Phys.* **28** (1962) 870.

[20] H. Georgi and C. Jarlskog, *A new lepton-quark mass relation in a unified theory*, *Phys. Lett.* **B 86** (1979) 297.

JHEP09(2003)028